Acoustic transparency of the chain-chain interface

Vitaly A. Kuzkin
Institute for Problems in Mechanical Engineering RAS, Saint Petersburg, Russia
and Peter the Great Saint Petersburg Polytechnical University, Saint Petersburg, Russia

(Received 23 February 2023; accepted 30 May 2023; published 28 June 2023)

We study propagation of wave packets through the interface between two dissimilar harmonic chains with on-site potentials (e.g., chains lying on elastic foundations). An expression for the transmission coefficient, relating energies of the incident and transmitted wave packets is derived using two different approaches. Without elastic foundation, the transmission coefficient monotonically decreases with increasing wave frequency. We show that by adding elastic foundations, one can qualitatively change this dependence and make it nonmonotonic or even increasing. Moreover, in some cases, the interface is totally transparent (the transmission coefficient is equal to unity at some frequency) if at least one of the chains has the elastic foundation. Presented results may serve for manipulation of the transmission coefficient and corresponding interfacial thermal resistance in low-dimensional nanosystems.

DOI: 10.1103/PhysRevE.107.065004

I. INTRODUCTION

Modeling of propagation of waves through the interface between two media with different properties is a long standing problem. Pioneering solutions of this problem have been obtained by Rayleigh for acoustic waves [1]. Since acoustic waves are dispersionless, the transmission coefficient, relating energies of incident and transmitted waves, depends on the ratio of acoustic impedances (product of density and sound speed) only. In systems with dispersion, the transmission coefficient also depends on frequency of the waves. This dependence can be efficiently demonstrated and analyzed using simple discrete models, which are always dispersive.

Current interest to analysis of wave propagation in discrete systems is caused, in particular, by active investigation of heat transfer in low-dimensional systems at nanoscale [2–6]. Peculiarities of heat transfer in nanoscale systems, such as quasiballistic [6,7] and anomalous [2–4] regimes of heat transfer, presence of several temperatures [8–10], heat waves [11], peculiar behavior of entropy [12], thermal echo [13], ballistic resonance [7] etc., make them perfect candidates for development of new devices for manipulation of thermal energy (e.g., thermal diodes [14,15]). One of the barriers to the use of unique thermal properties of nanosystems is the Kapitsa interfacial resistance [16], which is directly related to reflection of waves, carrying thermal energy, from the interface. We refer to the review [17] for analysis of recent progress in investigation of the Kapitsa resistance. Keeping the Kapitsa resistance in mind, we will focus on the simpler problem of propagation of wave packets through the interface between two chains.

Propagation of waves through the interface between two chains has been studied in many works [18–29]. Calculation of the transmission coefficient is usually based on the ansatz approach (see, e.g., [18]), in which the solution in the form of three semi-infinite waves (incident, transmitted, and reflected) is considered. It is assumed that the waves have the same frequency. Substitution of the ansatzs into equations of motion for particles at the interface allows to find a relation between amplitudes of the three waves. Given that the amplitudes of the incident and transmitted waves are known, the average energy fluxes and corresponding transmission coefficient are calculated. In papers [18,19], the transmission coefficient for a chain with different masses and stiffness is calculated. Interface between diatomic chains is considered in papers [20,21]. Influence of the spring connecting two chains and masses of particles at the interface on the transmission coefficient are analyzed in papers [22,23]. The effect of structure of the interfacial layer between two chains on the transmission is discussed in papers [24–26]. Propagation of waves through different point defects in chains is considered, e.g., in paper [27]. It is shown, in particular, that under some conditions the waves propagate through the defect without reflection.

The motivation for the present paper is twofold. First, we focus on the effect of on-site potential (elastic foundation) on propagation of waves through the interface between two chains. To the best of our knowledge, this effect has not been studied systematically. The effect is particularly important for low-dimensional nanoscale systems (carbyne, nanowires, graphene, etc.), which are usually located at a substrate that can be modeled by an elastic foundation. We show that the elastic foundation qualitatively changes the frequency dependence of the transmission coefficient. In particular, under some conditions the interface becomes totally transparent (transmission coefficient is equal to unity at some frequency). This effect is further referred to as the *acoustic transparency*. It is realized if both stiffness of elastic foundations and particle masses are different. Second, we make a contribution to development of the energy dynamics approach, proposed in the recent paper [30]. In paper [30] it is shown that in homogeneous harmonic chains (with identical masses and stiffness) the total energy flux is conserved. Generalization of this result for the case of two-dimensional harmonic scalar lattices is carried out in paper [31]. In inhomogeneous chains, the flux satisfies a balance equation, similar to the equation of

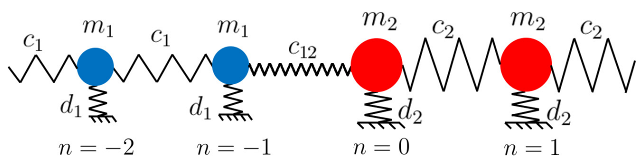

FIG. 1. The interface between chain 1 ($n<0$) and chain 2 ($n\geqslant 0$).

momentum balance. The balance equation is not closed, since it contains the unknown "force" acting on the wave packet. Therefore constitutive relations for this "force" are required. For chains with slowly varying properties these constitutive relations are derived in paper [30]. In the present paper, we show how the constitutive relations can be derived for the interface between two dissimilar chains, i.e., abrupt change of chain's parameters. Thus, we make a step toward analytical description of propagation of waves in inhomogeneous discrete media using the energy dynamics approach.

The paper is organized as follows. In Sec. II, we formulate equations of motion, describing dynamics of the two connected semi-infinite harmonic chains with harmonic on-site potentials (lying on linear elastic foundations). Initial conditions, corresponding to an incident wave packet, are discussed in Sec. III. In Sec. IV, frequency dependence of the transmission coefficient is obtained using the ansatz approach (for semi-infinite waves) and the energy dynamics approach [30] (for wave packets). In Sec. V, qualitative analysis of this dependence is presented. In Sec. VI, conditions for the acoustic transparency of the interface are derived. Influence of the way how spectra of the two chains intersect on the transmission coefficient is analyzed in Sec. VII.

II. EQUATIONS OF MOTION

We consider wave propagation in a system consisting of two connected semi-infinite chains on linear elastic foundations (with harmonic on-site potentials). Particles are numbered by integers n. In chain 1 the indices are negative, while in chain 2 they are nonnegative (see Fig. 1). The spring, connecting particles $n, n+1$, has half-integer number $n+\frac{1}{2}$. Masses of particles M_n, stiffness of springs $C_{n+\frac{1}{2}}$, and stiffness of elastic foundation D_n in chain 1 are equal to m_1, c_1, d_1, while in the chain 2 they are equal to m_2, c_2, d_2. The spring connecting the chains has stiffness c_{12}. Then

$$M_n = \begin{cases} m_1, & n<0, \\ m_2, & n\geqslant 0, \end{cases} \quad C_{n+\frac{1}{2}} = \begin{cases} c_1, & n<-1, \\ c_{12}, & n=-1, \\ c_2, & n\geqslant 0, \end{cases}$$
$$D_n = \begin{cases} d_1, & n<0, \\ d_2, & n\geqslant 0. \end{cases} \tag{1}$$

Using notation (1), we write equations of motion for all particles in the same form:

$$M_n \dot{v}_n = F_{n+\frac{1}{2}} - F_{n-\frac{1}{2}} - D_n u_n, \quad F_{n+\frac{1}{2}} = C_{n+\frac{1}{2}} \varepsilon_{n+\frac{1}{2}},$$
$$\varepsilon_{n+\frac{1}{2}} = u_{n+1} - u_n, \quad v_n = \dot{u}_n. \tag{2}$$

Initial conditions for the equations (2), corresponding to a wave packet, traveling from chain 1 to chain 2, are discussed in the next section.

The dispersion relations for chains 1 and 2 have the form

$$\omega_i^2(k_i) = \frac{d_i}{m_i} + \frac{4c_i}{m_i}\sin^2\frac{k_i}{2}, \quad k_i \in [0; 2\pi], \quad i=1,2. \tag{3}$$

The frequencies (3) satisfy inequalities

$$\frac{d_i}{m_i} \leqslant \omega_i^2 \leqslant \frac{4c_i + d_i}{m_i}. \tag{4}$$

Group velocities, corresponding to the dispersion relations (3), are given by

$$g_i(k_i) = a\frac{d\omega_i}{dk_i} = \frac{ac_i \sin k_i}{m_i \omega_i(k_i)}, \tag{5}$$

where a is the equilibrium distance between particles. Excluding the wave number k_i from (5), we obtain

$$g_i(\omega) = \frac{a}{2\omega}\sqrt{\left(\omega^2 - \frac{d_i}{m_i}\right)\left(\frac{4c_i + d_i}{m_i} - \omega^2\right)}. \tag{6}$$

This formula is valid for frequencies, satisfying the inequality (4), otherwise we set $g_i = 0$. For $d_i = 0$ the group velocity is equal to zero at the maximum frequency, while for $d_i \neq 0$ it vanishes at both minimum and maximum frequencies, given by (4).

III. INITIAL CONDITIONS

In this section, we discuss the initial conditions, corresponding to a wave packet with frequency Ω and a slowly changing envelope, traveling from chain 1 toward the interface. Due to Rayleigh's reciprocity theorem [32], the fraction of energy transmitted through the interface is independent on the direction of motion of the wave packet. Therefore it is sufficient to solve the problem (calculate the transmission coefficient) for wave packets traveling form chain 1 to chain 2.

To specify the initial conditions we use the following approximate solution of equations of motion for chain 1 [33,34]:

$$u_n = A(\beta na, \beta t)\sin(k_1 n - \Omega t), \quad |\beta| \ll 1. \tag{7}$$

Here β is a small parameter, $A(\beta x, \beta t)$ is a slowly changing envelope of the wave packet, where x is the coordinate, equal to na at particle positions in the undeformed chain. The expression (7) is substituted into equations of motion for chain 1. The equations are expanded into series with respect to β. Setting zero and first order terms equal to zero, we obtain

$$\Omega^2 - \frac{d_1}{m_1} - \frac{4c_1}{m_1}\sin^2\frac{k_1}{2} = 0, \quad \frac{\partial A}{\partial \beta t} = -g_1 \frac{\partial A}{\partial \beta x}, \tag{8}$$

where g_1 is the group velocity, corresponding to the wave number k_1. It is seen that the equations (8) are satisfied, provided that the frequency Ω is related to the wave number k_1 by the dispersion relation (3), while the envelope A travels with the group velocity, i.e., $A = A(\beta(x - g_1 t))$. Then the approximate solution (7) takes the form

$$\begin{aligned} u_n &\approx A(\beta(na - g_1 t))\sin(k_1 n - \Omega t), \\ v_n &\approx \dot{A}\sin(k_1 n - \Omega t) - \Omega A\cos(k_1 n - \Omega t). \end{aligned} \tag{9}$$

The solution remains accurate at time scale $\Omega t \sim \beta^{-1}$, while at larger time scale of the order β^{-2} the dispersion causes changing of the envelope's shape [33,34]. The approximate solution (9) allows to specify the wave packet with a desired envelope and to make sure that the envelope does not change significantly before reaching the interface.

In our numerical simulations, the initial displacements and velocities for chain 1 ($n < 0$) are specified using formula (9) at $t = 0$ with the Gaussian envelope A such that

$$\begin{aligned} u_n &= B_n \sin(k_1 n), \quad B_n = U_0 \exp\left(-\frac{\beta^2}{2}(n-n_0)^2\right), \\ v_n &= -B_n\left[\Omega \cos(k_1 n) - \frac{\beta^2 g_1}{a}(n-n_0)\sin(k_1 n)\right], \end{aligned} \tag{10}$$

where U_0 is the amplitude of displacements in the wave packet; $n_0 a < 0$ is the initial coordinate of the wave packet's center. For chain 2 ($n \geqslant 0$), zero initial conditions are used.

We note that since formula (10) is based on the approximate solution, it generates both the main wave packet propagating to the right and a small reverse wave packet propagating to the left. However, the amount of energy in the reverse packet is small and it decreases as $\beta \to 0$. To avoid the reverse wave packet one can use the approach described in paper [35]. In [35] the initial displacements are specified according to the first formula from (10). These displacements are then expanded using normal modes. The amplitudes of normal modes are used to specify the velocities such that all energy propagates in one direction and the reverse wave packet is absent. However, since the reverse wave packet has small energy, we have chosen the initial conditions (10) for simplicity.

Under initial conditions (10), all energy of the system is initially concentrated in the incident wave packet (in chain 1). At the interface, the incident wave packet is split into transmitted and reflected wave packets. Further we derive analytical expressions for the transmission coefficient, relating energies of these wave packets (see, e.g., Sec. IV B). In analytics, the transmission coefficient is obtained in the limit $\beta \to 0$. In this case, the transmission coefficient is independent of the particular shape of the wave packet's envelope.

IV. CALCULATION OF THE TRANSMISSION COEFFICIENT

In this section, we derive the expressions for the transmission coefficient using the ansatz approach (for semi-infinite waves) and the energy dynamics approach (for wave packets).

A. Ansatz approach

We start with derivation of the expression for the transmission coefficient using the particular solution of equations of motion (2) in the form of incident, reflected, and transmitted semi-infinite harmonic waves (see, e.g., [18,36]). Frequencies of the waves are equal, while their amplitudes are chosen such that the equations of motion for the interfacial particles -1 and 0 are satisfied. This solution does not satisfy the initial conditions (10), corresponding to a wave packet. However, we show below that the transmission coefficient, derived from this solution, coincides with the transmission coefficient, obtained for the wave packet, provided that the wave packet is sufficiently wide [i.e., $\beta \to 0$ in formula (10)].

Following [18,36], we seek the solution of the equations of motion (2) in the form of three harmonic waves having the same frequency Ω:

$$u_n = \begin{cases} A_I e^{\mathrm{i}(\Omega t - k_1 n)} + A_R e^{\mathrm{i}(\Omega t + k_1 n)}, & n < 0, \\ A_T e^{\mathrm{i}(\Omega t - k_2 n)}, & n \geqslant 0, \end{cases} \tag{11}$$

where i is the imaginary unit; $m_i \Omega^2 = d_i + 4c_i \sin^2 \frac{k_i}{2}$; A_I, A_R, A_T are amplitudes of the incident, reflected, and transmitted waves respectively; k_1, k_2 are wave numbers, corresponding to the frequency Ω. We limit ourselves by the case when waves with frequency Ω can propagate in both chains. Then k_1 and k_2 are real. The case of imaginary wave number k_2, corresponding to the total reflection from the interface and exponentially decaying solution in chain 2, is beyond the scope of the present paper.

For any A_I, A_R, A_T, the solution (11) satisfies equations of motion (2) for all particles except for the interface, i.e., for $n = -1$ and $n = 0$. Equations of motion for particles -1, 0 yield the relation between the amplitudes. These equations have the form

$$\begin{aligned} m_1 \ddot{u}_{-1} &= c_{12}(u_0 - u_{-1}) + c_1(u_{-2} - u_{-1}) - d_1 u_{-1}, \\ m_2 \ddot{u}_0 &= c_{12}(u_{-1} - u_0) + c_2(u_1 - u_0) - d_2 u_0. \end{aligned} \tag{12}$$

Substituting the solution (11) into equations (12), and using the dispersion relation in the form $c_i(e^{\mathrm{i}k_i} + e^{-\mathrm{i}k_i}) = 2c_i + d_i - m_i\Omega^2$, we obtain

$$\begin{aligned} (c_{12} - c_1)\big(A_I e^{\mathrm{i}k_1} + A_R e^{-\mathrm{i}k_1}\big) + c_1(A_I + A_T) &= c_{12} A_T, \\ \big[c_2(e^{\mathrm{i}k_2} - 1) + c_{12}\big] A_T &= c_{12}\big(A_I e^{\mathrm{i}k_1} + A_R e^{-\mathrm{i}k_1}\big). \end{aligned} \tag{13}$$

The system of equations (13) after some transformations yields

$$\frac{A_T}{A_I} = \frac{2\mathrm{i}c_{12}\sin k_1}{c_{12}(1 - e^{-\mathrm{i}k_1}) + c_2(e^{\mathrm{i}k_2} - 1)(1 + e^{-\mathrm{i}k_1}(c_{12} - c_1)/c_1)}. \tag{14}$$

We further focus on the case $c_{12} = c_1$ unless otherwise stated. This case is chosen for several reasons. First, it leads to the simplest expression for the transmission coefficient. Second, our results combined with Rayleigh's reciprocity theorem [32] show that the transmission coefficient for $c_{12} = c_1$ coincides with the transmission coefficient for $c_{12} = c_2$. Third, our main result, namely transparency of the interface, is observed when all stiffnesses are equal, i.e., $c_1 = c_2 = c_{12}$ (see section VI B). Since the frequencies of incident and transmitted waves are equal then the dispersion relations for chains 1 and 2 yield

$$c_1 - c_2 = \frac{1}{2}\Big[(m_1 - m_2)\Omega^2 + d_2 - d_1 + 2(c_1 \cos k_1 - c_2 \cos k_2)\Big]. \tag{15}$$

Substituting (15) into (14) and using the first equation from (13), we obtain

$$\begin{aligned} \frac{A_T}{A_I} &= \frac{4\mathrm{i}c_1 \sin k_1}{(m_1 - m_2)\Omega^2 + d_2 - d_1 + 2\mathrm{i}(c_1 \sin k_1 + c_2 \sin k_2)}, \\ A_I + A_R &= A_T. \end{aligned} \tag{16}$$

Thus, amplitudes of incident, transmitted, and reflected waves are related by formula (16).[1] Since energy fluxes and energy densities in the waves are proportional to absolute values of the amplitudes squared, the formula (16) allows to calculate the transmission coefficient.

According to the solution (11), energies carried by the incident, transmitted, and reflected waves are infinite. Therefore, for semi-infinite waves we define the transmission and reflection coefficients T and R in terms of fluxes rather than energies:

$$T = \frac{h_T}{h_I}, \quad R = 1 - T, \tag{17}$$

where h_I and h_T are average[2] fluxes in the incident and transmitted waves, respectively. This formula can be interpreted as follows. During the period $2\pi/\Omega$, the incident wave brings toward the interface the amount of energy $2\pi h_I/\Omega$, while the amount of transmitted energy during the same time is $2\pi h_T/\Omega$. The ratio of these energies is equal to the transmission coefficient.

Using formula (A6) for the average flux in a harmonic wave, we obtain

$$T = \frac{m_2 g_2 |A_T|^2}{m_1 g_1 |A_I|^2}. \tag{18}$$

Substitution of (16) into (18) yields

$$T = \frac{16\Omega^2 m_1 m_2 g_1 g_2}{4\Omega^2(m_1 g_1 + m_2 g_2)^2 + a^2\big((m_1 - m_2)\Omega^2 + d_2 - d_1\big)^2}, \tag{19}$$

where $g_i = g_i(\Omega)$. We note that formula (19) is symmetric with respect to change of indices 1,2.

Analysis of frequency dependence of the transmission coefficient is presented below in Secs. V–VI. Since formula (19) is derived from the exact solution (11), it is further used as a benchmark.

B. Energy dynamics

In this subsection, we derive the expression for the transmission coefficient using the energy dynamics approach [30]. In contrast to the previous subsection, here we deal with wave packets rather than the semi-infinite waves. The key quantity of interest is the total energy flux in the system. In the homogeneous case (for $m_1 = m_2, c_1 = c_2 = c_{12}, d_1 = d_2$), the total flux is conserved under arbitrary initial conditions [30] [see also formula (23)]. In the inhomogeneous case (in the presence of the interface), the total flux is generally not conserved for two reasons. First, the flux in chain 1 changes sign due to reflection. Second, since group velocities in chains 1 and 2 are different, then the energy is transferred in them at different speeds. Therefore, evolution of the total flux in time is closely related to reflection. To describe the evolution, we derive the balance equation for the total energy flux. The right hand side of this equation can be interpreted as a "force," acting on a wave packet. The force depends on the difference between parameters of chains 1 and 2 and on motion of particles -1 and 0, located at the interface. Using the balance equation and additional "constitutive" relations, we calculate the transmission coefficient.

1. Balance of the total energy flux

We derive the balance equation for the total energy flux in the system, described by equations of motion (2). Following [30], we define the total energy flux h and the local flux $h_{n+\frac{1}{2}}$ as

$$h = \sum_{n=-\infty}^{+\infty} h_{n+\frac{1}{2}}, \quad h_{n+\frac{1}{2}} = -\frac{a}{2} F_{n+\frac{1}{2}}(v_n + v_{n+1}). \tag{20}$$

Calculating the derivative of the local flux $h_{n+\frac{1}{2}}$ with respect to time

$$\begin{aligned}\dot{h}_{n+\frac{1}{2}} = &-\frac{a}{2} C_{n+\frac{1}{2}}\left(v_{n+1}^2 - v_n^2\right)\\ &-\frac{a}{2} F_{n+\frac{1}{2}}\left(\frac{F_{n+\frac{1}{2}}}{M_n} - \frac{F_{n+\frac{1}{2}}}{M_{n+1}} + \frac{F_{n+\frac{3}{2}}}{M_{n+1}} - \frac{F_{n-\frac{1}{2}}}{M_n}\right.\\ &\left. - \frac{D_{n+1}u_{n+1}}{M_{n+1}} - \frac{D_n u_n}{M_n}\right)\end{aligned} \tag{21}$$

and summing (21) with respect to all particles, we obtain

$$\begin{aligned}\dot{h} = &-\frac{a}{2}(c_{12} - c_2)\left(v_0^2 - \frac{d_2 u_0^2}{m_2}\right)\\ &-\frac{a}{2}(c_1 - c_{12})\left(v_{-1}^2 - \frac{d_1 u_{-1}^2}{m_1}\right)\\ &+\frac{a(m_1 - m_2)}{2m_1 m_2} c_{12}^2 \varepsilon_{-\frac{1}{2}}^2 + \frac{a c_{12}}{2}\left(\frac{d_1}{m_1} - \frac{d_2}{m_2}\right) u_0 u_{-1}.\end{aligned} \tag{22}$$

This exact formula is valid under arbitrary initial conditions.

To reduce the number of parameters, we further focus on the particular case $c_{12} = c_1$ (see discussion in Sec. IV A). Substituting $c_{12} = c_1$ into the formula (22), yields

$$\begin{aligned}\dot{h} = \mathcal{F}(t), \quad \mathcal{F} = &\frac{a}{2}(c_2 - c_1)\left(v_0^2 - \frac{d_2}{m_2} u_0^2\right)\\ &+\frac{a(m_1 - m_2)}{2m_1 m_2} c_1^2 \varepsilon_{-\frac{1}{2}}^2 + \frac{a c_1}{2}\left(\frac{d_1}{m_1} - \frac{d_2}{m_2}\right) u_0 u_{-1}.\end{aligned} \tag{23}$$

Formula (23) shows that changes of the total flux are caused by the "force" $\mathcal{F}$, which depends on differences between parameters of the chains and on motion of the interfacial particles -1 and 0. If the particles don't move (e.g., before and after the reflection) then the force is equal to zero and the flux remains constant. Here and below we assume that there is no localization of energy at the interface, i.e., all energy is either transmitted or reflected. Investigation of possibility of localization is beyond the scope of the present paper. We refer to, e.g., works [37–42] for analysis of continuum and discrete systems with localization.

We further use the balance law (23) to calculate the amount of energy transmitted through the interface.

[1] The particular case of (16) for $m_1 = m_2$, $d_1 = d_2 = 0$ is obtained in the book [36].

[2] The averaging is carried out over the period, which is identical for incident, reflected, and transmitted waves.

2. Transmission coefficient

To define the transmission coefficient in the framework of the energy dynamics approach, we denote energies of chains 1,2 at time t as $E_1(t)$ and $E_2(t)$. Then the transmission coefficient T is defined by

$$T = \frac{E_2(\infty)}{E}, \quad E_2(\infty) = \lim_{t\to\infty} E_2(t), \tag{24}$$

where $E = E_1 + E_2$ is the total energy of the system, which is equal to the energy of the incident wave packet. We note that this definition formally differs from the previous definition (17). The definition (24) is natural for wave packets, while it is inapplicable to semi-infinite waves. In turn, the definition (17) is inapplicable to wave packets.

To find the frequency dependence of the transmission coefficient, we integrate equation (23) over time:

$$h(\infty) - h(0) = \int_0^\infty \mathcal{F} dt. \tag{25}$$

To represent all quantities in this formula in terms of energies of incident, transmitted, and reflected wave packets, we assume that the energy is transferred to chain 2 by a wave packet with frequency Ω and unknown envelope $B(\beta na, \beta t)$:

$$u_n = B(\beta na, \beta t)\sin(k_2 n - \Omega t), \quad n \geqslant 0, \quad |\beta| \ll 1. \tag{26}$$

In Appendix A it is shown that the flux, corresponding to the initial conditions (10) for small β, has the form

$$h(0) \approx E g_1(\Omega), \tag{27}$$

where $g_1(\Omega)$ is the group velocity for chain 1, corresponding to the frequency Ω. Under assumption (26), a similar expression is valid for the total flux in chain 2, i.e., the total flux is equal to $E_2(\infty)g_2(\Omega)$. We also assume that the reflected wave packet has the frequency Ω. Then the total flux at large times is given by

$$h(\infty) \approx E_2(\infty)g_2(\Omega) - E_1(\infty)g_1(\Omega). \tag{28}$$

Substitution of formulas (27) and (28) into (25) yields

$$E_2(\infty)g_2(\Omega) - \big(E + E_1(\infty)\big)g_1(\Omega) \approx \int_0^\infty \mathcal{F} dt. \tag{29}$$

The last and the most complicated step toward calculation of the transmission coefficient is to represent the r.h.s. in (29) in terms of energies. In Appendix B it is shown that

$$\begin{aligned}
&\int_0^\infty \mathcal{F} dt \approx G(\Omega)E_2(\infty),\\
&G = \frac{a^2}{2g_2\Omega^2}\left[\frac{(2m_1 - m_2)c_2 - c_1 m_1}{m_1 m_2}\left(\Omega^2 - \frac{d_2}{m_2}\right)\right.\\
&\qquad \left. + \frac{1}{2}\left(\frac{2c_1 + d_2}{m_2} - \Omega^2\right)\left(\frac{d_1}{m_1} - \frac{d_2}{m_2}\right)\right].
\end{aligned} \tag{30}$$

Formula (30) is derived by combining the solution (26) with equations of energy balance and dynamics equations for the interfacial particles. This allows to relate $\mathcal{F}$ with the envelope function $B(\beta na, \beta t)$, which in turn is related to the energy E_2 (see Appendix B for details).

Substituting (30) into (29), dividing both parts by E, and using the definition of the transmission coefficient (24), we finally obtain

$$T = \frac{2g_1(\Omega)}{g_1(\Omega) + g_2(\Omega) - G(\Omega)}. \tag{31}$$

We note that formulas (19) and (31) are obtained by entirely different means and using formally different definitions (17), (24) for the transmission coefficient. Formula (19) is exact because it is derived using the exact solution (11). Derivation of the formula (31) involves several assumptions and approximations. However, the accuracy of these approximations increases with decreasing β (increasing width of the wave packet). Therefore the transmission coefficients, calculated by formulas (19) and (31), coincide in all cases we have considered.[3]

Thus, the energy dynamics approach allows to calculate the transmission coefficient. Although it is less straightforward than the "ansatz" approach, we expect that the energy dynamics can be used when there is no exact solution like (11).

V. QUALITATIVE AND DIMENSIONAL ANALYSIS

In this section, we discuss qualitative features of the frequency dependence of the transmission coefficient $T(\Omega)$, given by formula (19).

Since the transmission coefficient is dimensionless, it depends only on the dimensionless parameters of the problem. To introduce the dimensionless frequency, we use the fact that the transmission coefficient is not equal to zero only if the waves with frequency Ω can propagate in both chains 1 and 2. In other words, Ω should satisfy the relations

$$\begin{aligned}
&\Omega_{\text{low}} \leqslant \Omega \leqslant \Omega_{\text{high}}, \quad \Omega_{\text{low}}^2 = \max\left(\frac{d_1}{m_1}, \frac{d_2}{m_2}\right),\\
&\Omega_{\text{high}}^2 = \min\left(\frac{4c_1 + d_1}{m_1}, \frac{4c_2 + d_2}{m_2}\right).
\end{aligned} \tag{32}$$

Using formula (32), we introduce the dimensionless frequency

$$\tilde{\Omega}^2 = \frac{\Omega^2 - \Omega_{\text{low}}^2}{\Omega_{\text{high}}^2 - \Omega_{\text{low}}^2}. \tag{33}$$

Then the transmission is possible provided that $\tilde{\Omega}^2 \in [0; 1]$. Formula (33) allows, in particular, to plot frequency dependencies of the transmission coefficient for different values of parameters on a single graph.

The transmission coefficient also depends on the mass ratio m_1/m_2, stiffness ratio c_1/c_2, ratio of stiffness of elastic foundations d_1/d_2, and on d_1/c_1 (for $c_{12} = c_1$). Therefore, in general, it is a function of five parameters:

$$T = T\left(\tilde{\Omega}^2, \frac{m_1}{m_2}, \frac{c_1}{c_2}, \frac{d_1}{d_2}, \frac{d_1}{c_1}\right). \tag{34}$$

We show below that the number of parameters can be reduced at least by one [see formulas (57), (67)].

[3]Though in the most general case we were not able to derive (19) from (31) or vice versa, we were also not able to find the case when the two definitions yield different values of T.

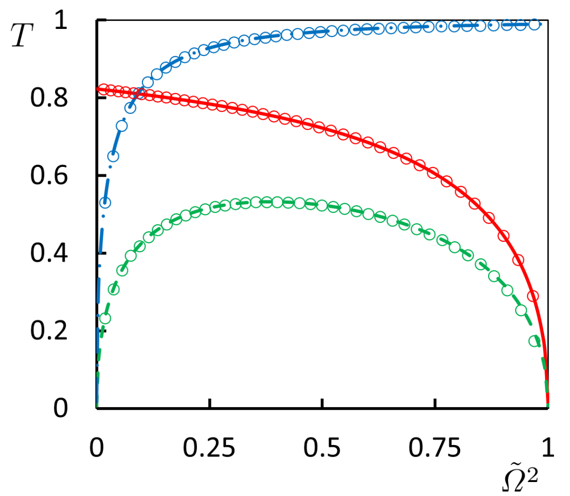

FIG. 2. Three qualitatively different frequency dependencies of the transmission coefficient T, calculated by formulas (19) and (31). Solid red line—case (35) for $m_2/m_1 = 2$, $c_2/c_1 = 3$, $d_2/d_1 = 2$, $c_1/d_1 = 1$; dashed green line— the second case from (36) for $m_2/m_1 = 3$, $c_2/c_1 = 2$, $d_2/d_1 = 1/2$, $c_1/d_1 = 1$; dash dotted blue line—case (37) for $m_2/m_1 = 2/3$, $c_2/c_1 = 1$, $d_2/d_1 = 0$, $c_1/d_1 = 1/2$. Numerical results are shown by circles.

Consider qualitative features of frequency dependence of the transmission coefficient. The dependence is determined by the way how spectra (passbands[4]) of chains 1 and 2 intersect with each other. Three qualitatively different dependencies $T(\Omega)$ are shown in Fig. 2. These dependencies correspond to the following three cases.

Case 1. Equal minimal frequencies:

$$\frac{d_1}{m_1} = \frac{d_2}{m_2}. \tag{35}$$

Under condition (35), the transmission coefficient monotonically decreases with increasing frequency[5] (see solid line in Fig. 2). In particular, this condition is satisfied in the absence of elastic foundation ($d_1 = d_2 = 0$) and for chains with identical spectra $m_1/m_2 = c_1/c_2 = d_1/d_2$. These cases are further analyzed in Secs. VII B 1 and VII D.

Case 2. Intersecting or nested spectra with

$$\left[\begin{array}{l} \dfrac{d_1}{m_1} \neq \dfrac{d_2}{m_2}, \quad \dfrac{4c_1 + d_1}{m_1} \neq \dfrac{4c_2 + d_2}{m_2}, \\[2mm] \dfrac{d_1}{m_1} \neq \dfrac{d_2}{m_2}, \quad \dfrac{4c_1 + d_1}{m_1} = \dfrac{4c_2 + d_2}{m_2}, \quad c_1 \neq c_2. \end{array}\right. \tag{36}$$

Under conditions (36), the transmission coefficient first monotonically increases from zero at $\tilde{\Omega} = 0$ to the maximum value and then monotonically decreases toward zero at $\tilde{\Omega} = 1$ (see dashed line in Fig. 2). The case of nested spectra is further analyzed in Sec. VII B, while the case of intersecting spectra is analyzed in Sec. VII C.

[4]By spectra or passbands we mean intervals $[d_1/m_1; (4c_1 + d_1)/m_1]$, $[d_2/m_2; (4c_2 + d_2)/m_2]$.

[5]Excluding the trivial case when left and right parts on the chains have identical parameters. In the latter case, the transmission coefficient is equal to 1 for all frequencies inside the spectrum.

Case 3. Equal maximal frequencies and equal stiffnesses:

$$\frac{d_1}{m_1} \neq \frac{d_2}{m_2}, \quad \frac{4c_1 + d_1}{m_1} = \frac{4c_2 + d_2}{m_2}, \quad c_1 = c_2. \tag{37}$$

Under conditions (37), the transmission coefficient monotonically increases from zero at $\tilde{\Omega} = 0$ toward the maximum value at $\tilde{\Omega} = 1$ (see dash dotted line in Fig. 2). This case is further analyzed in Sec. VII B 2.

To check formulas (19) and (31) for the transmission coefficient, we solve the equations of motion (2) with initial conditions (10) numerically using the leap-frog integration scheme with time step of $0.05/\Omega_{\text{high}}$. The two connected chains, consisting of 1500 particles each, are considered. The initial wave packet is given by (10) with $\beta = 0.02$ and $n_0 = -4/\beta$. In simulations, the total energies $E_1(t)$, $E_2(t)$ of the two chains are computed. After the reflection, these energies become constant in time. These constant values are used for calculation of the transmission coefficient by formula (24). Numerical results are presented by circles in Fig. 2. It is seen that the numerical and analytical results practically coincide. Our simulations also show that the transmission coefficient, generally, depends on β. If the envelope of the wave packet is narrow (β is large), then the numerical results deviate from the analytical solution (19), because the latter formally corresponds to the case $\beta = 0$. The deviation is larger at higher frequencies. The difference between numerical and analytical solutions decreases as β tends to zero.

Thus, in the absence of elastic foundation (or for chains on elastic foundations having identical minimal frequencies), the frequency dependence of the transmission coefficient is monotonically decreasing. Adding the elastic foundation, one can qualitatively change this dependence and make it nonmonotonic or monotonically increasing. Moreover, in the next section we show that in some cases the elastic foundation makes the interface totally transparent.

VI. TOTAL ACOUSTIC TRANSPARENCY

In this section, we discuss the phenomenon of acoustic transparency, i.e., propagation of waves through the interface without reflection ($T = 1$). To obtain the conditions of acoustic transparency, we write the following expression for the reflection coefficient R using formula (19):

$$R = 1 - T = \frac{4\Omega^2(m_1 g_1 - m_2 g_2)^2 + a^2\big((m_1 - m_2)\Omega^2 + d_2 - d_1\big)^2}{4\Omega^2(m_1 g_1 + m_2 g_2)^2 + a^2\big((m_1 - m_2)\Omega^2 + d_2 - d_1\big)^2}. \tag{38}$$

Since both terms in the numerator are nonnegative, the reflection coefficient vanishes ($R = 0$) only if

$$m_1 g_1(\Omega) = m_2 g_2(\Omega), \quad (m_1 - m_2)\Omega^2 + d_2 - d_1 = 0. \tag{39}$$

The second equation is satisfied at the frequency

$$\Omega^2 = \Omega_t^2 = \frac{d_1 - d_2}{m_1 - m_2}. \tag{40}$$

Therefore, Ω_t is further referred to as the *frequency of transparency*.

Substitution of (40) into the first equation from (39) after algebraic transformations, yields $(c_1 - c_2)(d_1 m_2 - d_2 m_1) = 0$. Then the acoustic transparency is possible at frequency Ω_t provided that either stiffnesses are equal ($c_1 = c_2$) or the minimal frequencies are equal ($d_1/m_1 = d_2/m_2$). These two cases are analyzed below.

A. Equal minimal frequencies

In the case of equal minimal frequencies $d_1/m_1 = d_2/m_2$ (including the case when there are no elastic foundations $d_1 = d_2 = 0$), the formula (40) for Ω_t reduces to

$$\Omega_t^2 = \frac{d_1}{m_1} = \frac{d_2}{m_2}. \tag{41}$$

Then both numerator and denominator of the expression (38) are equal to zero at $\Omega = \Omega_t$. Calculating the limit $\Omega \to \Omega_t$, we show that the transmission coefficient is given by formula (52). From this formula it follows that the total transmission is achieved provided that

$$\Omega^2 = \Omega_t^2 = \frac{d_1}{m_1} = \frac{d_2}{m_2}, \quad m_1 c_1 = m_2 c_2. \tag{42}$$

These conditions include the case when there are no elastic foundations ($d_1 = d_2 = 0$).

Consider frequency dependence of the transmission coefficient. Using formula (42) and assuming that $c_1/m_1 < c_2/m_2$, we obtain[6]

$$T = \frac{2\sqrt{(1-\tilde{\Omega}^2)(\gamma_*^2 - \tilde{\Omega}^2)}}{\gamma_* - \tilde{\Omega}^2 + \sqrt{(1-\tilde{\Omega}^2)(\gamma_*^2 - \tilde{\Omega}^2)}}, \quad \gamma_* = \frac{m_1}{m_2} = \frac{d_1}{d_2} = \frac{c_2}{c_1} > 1. \tag{43}$$

A similar expression for $c_1/m_1 > c_2/m_2$ can be obtained by permutation of the indices 1,2 in the expression for γ_*. The transmission coefficient (43) is equal to unity at $\tilde{\Omega} = 0$. For large γ_*, the frequency dependence of the transmission coefficient tends to a limiting curve:

$$T = \frac{2\sqrt{1-\tilde{\Omega}^2}}{1+\sqrt{1-\tilde{\Omega}^2}}. \tag{44}$$

The dependence (43) for different values of γ_* is shown in Fig. 3. It is seen that, as expected, the transmission coefficient is equal to 1 at $\tilde{\Omega} = 0$. For $0 < \tilde{\Omega} < 1$ the transmission coefficient decreases with increasing contrast in parameters γ_* and tends to the limiting curve (44).

Thus, in the case of equal minimal frequencies, the conditions of acoustic transparency are given by (42). However, we note that since the group velocities vanish at the minimal frequency (for $d_1 \neq 0$, $d_2 \neq 0$) then, strictly speaking, the waves with $\Omega = \Omega_t$ do not transport the energy. However, the transmission coefficient is still close to one in some vicinity of the minimal frequency.

[6]Note that formula (43) remains valid for $d_1 = d_2 = 0$. In this case $\gamma_* = m_1/m_2 = c_2/c_1$.

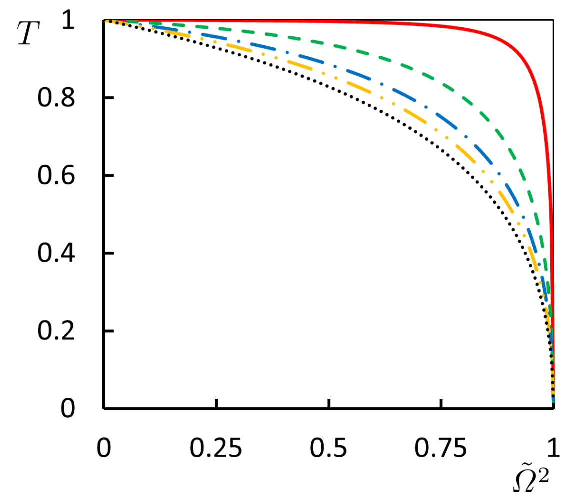

FIG. 3. Frequency dependence of the transmission coefficient T [formula (43)] for γ_* equal to 1.1 (solid line), 2 (dashed line), 4 (dash dotted line), and 8 (dash double dotted line) are shown. The dotted line shows the limiting case $\gamma_* \to \infty$, given by formula (44).

B. Equal stiffnesses

Consider the case of equal stiffnesses and different minimal and maximal frequencies, i.e. $c_1 = c_2 = c$, $d_1/m_1 \neq d_2/m_2$, and $(4c + d_1)/m_1 \neq (4c + d_2)/m_2$. Then the conditions (39) are satisfied and the total transmission is possible, provided that the frequency Ω_t belongs to spectra of the two chains, i.e.,

$$\Omega_{\text{low}} < \Omega_t < \Omega_{\text{high}}, \tag{45}$$

where $\Omega_{\text{low}}, \Omega_{\text{high}}$ are defined by (32). This condition is satisfied only in the case of nested spectra, considered in Sec. VII B. Rewriting the inequalities (45) in terms of parameters of the chains and taking into account equality of stiffnesses, we obtain the following conditions of acoustic transparency

$$\Omega^2 = \Omega_t^2 = \frac{d_1 - d_2}{m_1 - m_2}, \quad c_1 = c_2 = c, \quad 0 < \frac{m_2 d_1 - m_1 d_2}{4c(m_1 - m_2)} < 1. \tag{46}$$

The last formula in (46) is identical to the condition $0 < \tilde{\Omega}_t^2 < 1$, where $\tilde{\Omega}_t$ is the dimensionless frequency of transparency [see formula (49)]. We note that the interface can be transparent even if only one chain has the elastic foundation.

To explain the phenomenon of acoustic transparency, we show that under the conditions (46) the equations of motion (2) has the exact solution in the form of a harmonic wave, propagating in both chains. Substituting conditions (39) into formulas (15) and (16), and using expressions (5) for the group velocities, we obtain

$$A_I = A_T, \quad A_R = 0, \quad k_1 = k_2 = k_t. \tag{47}$$

Combining (47) with (11), we show that the equations of motion (2) has the exact solution

$$u_n = A_I e^{\mathrm{i}(\Omega_t t - k_t n)}, \quad \sin^2 \frac{k_t}{2} = \frac{m_2 d_1 - m_1 d_2}{4c(m_1 - m_2)}. \tag{48}$$

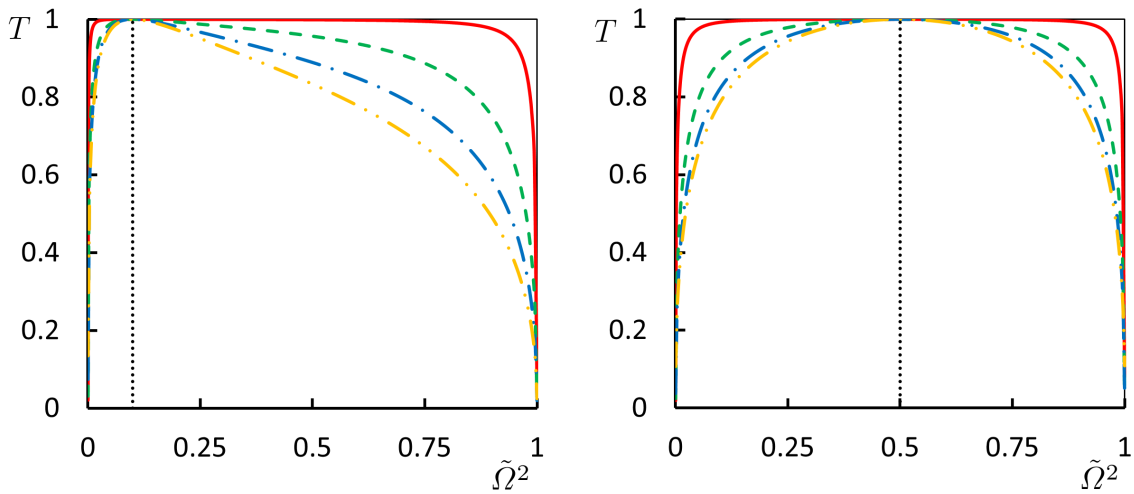

FIG. 4. Frequency dependence of the transmission coefficient T for $\tilde{\Omega}_t^2 = 0.1$ ($k_t = \pi/5$, left) and $\tilde{\Omega}_t^2 = 0.5$ ($k_t = \pi/2$, right). In both plots results for m_1/m_2 equal to 1.1 (solid line), 2 (dashed line), 4 (dash dotted line), and 8 (dash double dotted line) are shown. Vertical dotted lines correspond to $\tilde{\Omega} = \tilde{\Omega}_t$.

Here Ω_t is given by formula (46); the second formula for k_t follows from the dispersion relations (3) and equality of frequencies of the incident and transmitted waves. We note that the r.h.s. in the second formula in (48) is equal to the dimensionless frequency of transparency

$$\tilde{\Omega}_t^2 = \frac{m_2 d_1 - m_1 d_2}{4c(m_1 - m_2)} = \frac{\Omega_t^2 - \Omega_{\text{low}}^2}{\Omega_{\text{high}}^2 - \Omega_{\text{low}}^2}. \tag{49}$$

Thus, the harmonic wave with frequency Ω_t and wave number k_t propagates through the interface without reflection.

To illustrate the phenomenon of acoustic transparency, we consider the frequency dependence of the transmission coefficient under the conditions (46). The dependence is given by formula (58) with $c_1 = c_2$. The formula shows that the transmission coefficient depends on dimensionless frequency $\tilde{\Omega}$, mass ratio m_1/m_2, and dimensionless frequency of transparency $\tilde{\Omega}_t$. For example, we plot frequency dependence of the transmission coefficient for $\tilde{\Omega}_t^2 = 0.1$ ($k_t \approx \pi/5$) and $\tilde{\Omega}_t^2 = 0.5$ ($k_t = \pi/2$) at different mass ratios (see Fig. 4). As expected, the transmission coefficient decreases with increasing mass ratio, except for the frequency $\tilde{\Omega} = \tilde{\Omega}_t$, at which the interface is always transparent, i.e., $T = 1$.

To demonstrate changes of the wave packet when passing through the transparent interface, we plot the distribution of the local energy e_n before (at $t = 0$) and after (at $t = 3n_0 a/g_1$) the transmission (see Fig. 5). The local energy is defined as

$$e_n = \frac{1}{2}M_n v_n^2 + \frac{1}{4}C_{n-\frac{1}{2}}\varepsilon_{n-\frac{1}{2}}^2 + \frac{1}{4}C_{n+\frac{1}{2}}\varepsilon_{n+\frac{1}{2}}^2 + \frac{1}{2}D_n u_n^2. \tag{50}$$

Figure 5 shows that all energy is transmitted through the interface without reflection. Since chains 1 and 2 have different group velocities [in Fig. 5, $g_1(\Omega_t) = 2g_2(\Omega_t)$], spatial distribution of energy in the incident and transmitted wave packets is also different. The energy envelope in the transmitted wave packet is twice as high and twice as narrow as in the incident wave packet, while the total energies are equal.

We note that under the transparency conditions (46), the total energy flux is not conserved. As mentioned above, changes in the total energy flux are generally caused by two mechanisms: (i) changes in the sign of the flux in chain 1 due to reflection and (ii) changes of the group velocity from g_1 in chain 1 to g_2 in chain 2. Since in the case of acoustic transparency there is no reflection, changes of the energy flux are due to the second mechanism only.

Thus, the interface is transparent at $\Omega = \Omega_t$ even at high contrast of parameters (e.g., $m_1/m_2 = 8$). We note that in the vicinity of frequency Ω_t the transmission coefficient is close to unity and therefore the interface is almost transparent. The transmission coefficient is also close to unity for $c_1 \approx c_2$. Therefore, the effect of acoustic transparency is "robust" with respect to small variation of conditions (46).

VII. INFLUENCE OF SPECTRA INTERSECTION ON THE TRANSMISSION COEFFICIENT

In this section, we consider influence of the way how spectra of the chains intersect on frequency dependence of the transmission coefficient and analyze different particular cases.

A. Low- and high-frequency limits

In this subsection, we analyze the behavior of the transmission coefficient, given by formula (19), in the vicinity of the lowest and highest frequencies, Ω_{low} and Ω_{high}, defined by formula (32).

Low-frequency limit. We calculate the transmission coefficient at the lowest frequency Ω_{low}, at which the transmission is possible, i.e.,

$$T_{\text{low}} = \lim_{\Omega \to \Omega_{\text{low}}} T. \tag{51}$$

Substituting (19) into (51) and calculating the limit, we obtain

$$T_{\text{low}} = \begin{cases} \dfrac{4\sqrt{c_1 m_1 c_2 m_2}}{\left(\sqrt{c_1 m_1} + \sqrt{c_2 m_2}\right)^2}, & \dfrac{d_1}{m_1} = \dfrac{d_2}{m_2}, \\ 0, & \dfrac{d_1}{m_1} \neq \dfrac{d_2}{m_2}. \end{cases} \tag{52}$$

This formula is valid, in particular, for $d_1 = d_2 = 0$. It shows that the energy is totally transmitted through the interface

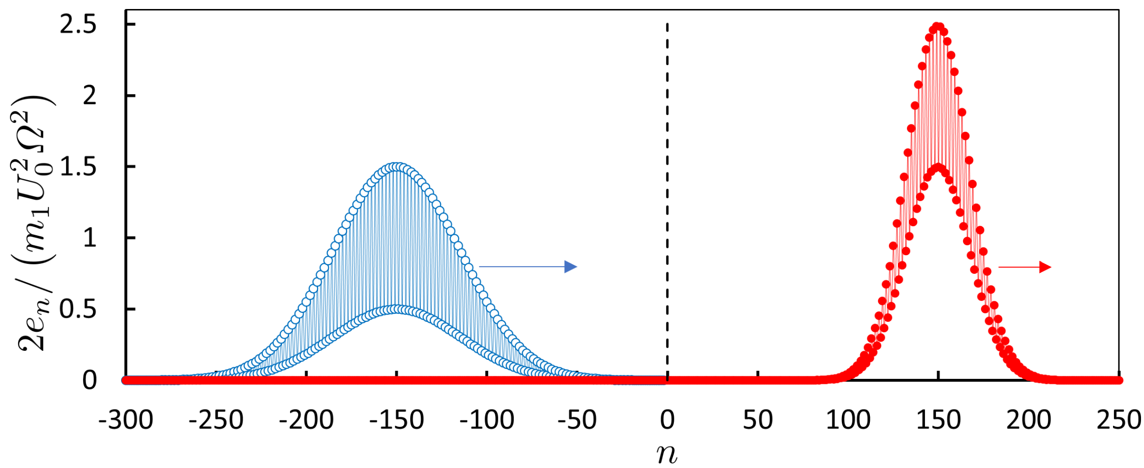

FIG. 5. Acoustic transparency of the interface at $\tilde{\Omega}^2 = \tilde{\Omega}_t^2 = 0.5$, $m_1/m_2 = 1/2$, $c_1 = c_2$, $d_1 = 0$, $d_2/c_2 = 2$. Local energies e_n for all particles at $t = 0$ (blue empty circles) and at $t = 3n_0a/g_1$ (red circles) are shown. No reflected wave is observed. Arrows show directions of the energy flux. Lengths of the arrows are proportional to the values of group velocities ($g_1 = 2g_2$).

($T_{\text{low}} = 1$) at the lowest frequency, provided that $m_1c_1 = m_2c_2$ (see Sec. VI A).

High-frequency limit. We calculate the transmission coefficient at the highest frequency Ω_{high} at which the transmission is possible, i.e.,

$$T_{\text{high}} = \lim_{\Omega\to\Omega_{\text{high}}} T. \tag{53}$$

Substituting (19) into (53) and calculating the limit, we obtain

$$T_{\text{high}} = \frac{4\sqrt{m_1m_2}}{\left(\sqrt{m_1}+\sqrt{m_2}\right)^2}, \tag{54}$$

for $(4c_1 + d_1)/m_1 = (4c_2 + d_2)/m_2$, $c_1 = c_2$, and $T_{\text{high}} = 0$ otherwise. For example, the formula (54) is valid for $m_2/m_1 = 2/3$, $c_2/c_1 = 1$, $d_2/d_1 = 0$, and $c_1/d_1 = 1/2$. The frequency dependence of the transmission coefficient for these values of parameters is shown by the dash dotted line in Fig. 2. For further analysis of this case see Sec. VII B 2.

B. Nested spectra

In the present subsection, we consider the case when the spectrum of chain 2 is inside the spectrum of chain 1 (or vice versa), i.e., either

$$\frac{d_1}{m_1} \leqslant \frac{d_2}{m_2} < \frac{4c_2+d_2}{m_2} \leqslant \frac{4c_1+d_1}{m_1} \tag{55}$$

or

$$\frac{d_2}{m_2} \leqslant \frac{d_1}{m_1} < \frac{4c_1+d_1}{m_1} \leqslant \frac{4c_2+d_2}{m_2}. \tag{56}$$

We focus on case (56). Similar results for case (55) can be obtained by permutation of indices. We show that the number of dimensionless arguments of the transmission coefficient in formula (34) can be reduced by one.

Using the frequency of transparency Ω_t, we show that the transmission coefficient depends on four parameters:

$$T = T\left(\tilde{\Omega}^2, \frac{m_1}{m_2}, \frac{m_1c_2}{m_2c_1}, \tilde{\Omega}_t^2\right),$$
$$\tilde{\Omega}_t^2 = \frac{\Omega_t^2 - \Omega_{\text{low}}^2}{\Omega_{\text{high}}^2 - \Omega_{\text{low}}^2} = \frac{d_1m_2 - d_2m_1}{4c_1(m_1-m_2)}. \tag{57}$$

The explicit form of the dependence (57) is given by the following formula:

$$T = \frac{4\frac{m_1}{m_2}\sqrt{\tilde{\Omega}^2(1-\tilde{\Omega}^2)}\, W}{\left[\frac{m_1}{m_2}\sqrt{\tilde{\Omega}^2(1-\tilde{\Omega}^2)}+W\right]^2 + \left(\frac{m_1}{m_2}-1\right)^2\left(\tilde{\Omega}^2-\tilde{\Omega}_t^2\right)^2},$$
$$W = \sqrt{\left[\frac{m_1c_2}{m_2c_1} + \left(1-\frac{m_1}{m_2}\right)\tilde{\Omega}_t^2 - \tilde{\Omega}^2\right]\left[\left(1-\frac{m_1}{m_2}\right)\tilde{\Omega}_t^2 + \tilde{\Omega}^2\right]}. \tag{58}$$

Formula (58) for $c_1 = c_2$ yields frequency dependence of the transmission coefficient in the case of acoustic transparency (see Sec. VI).

1. Equal minimal frequencies

We consider the case of equal minimal frequencies, i.e., $d_1/m_1 = d_2/m_2$. In particular, the presented results are valid for systems without elastic foundation ($d_1 = d_2 = 0$). It can be shown that $\tilde{\Omega}_t^2 = 0$ for $d_1/m_1 = d_2/m_2$ and formula (58) reduces to

$$T = \frac{4\sqrt{(1-\tilde{\Omega}^2)\left(\frac{m_1c_2}{m_2c_1}-\tilde{\Omega}^2\right)}}{\frac{m_1}{m_2}+\frac{c_2}{c_1}-2\tilde{\Omega}^2+2\sqrt{(1-\tilde{\Omega}^2)\left(\frac{m_1c_2}{m_2c_1}-\tilde{\Omega}^2\right)}}. \tag{59}$$

The maximum value of the transmission coefficient (59) is achieved at the lowest frequency (at $\tilde{\Omega} = 0$). The transmission coefficient monotonically decreases toward zero value at the highest frequency (at $\tilde{\Omega} = 1$). For illustration, frequency dependence of the transmission coefficient for $c_1 = c_2$ and different values of m_1/m_2 is shown in Fig. 6.

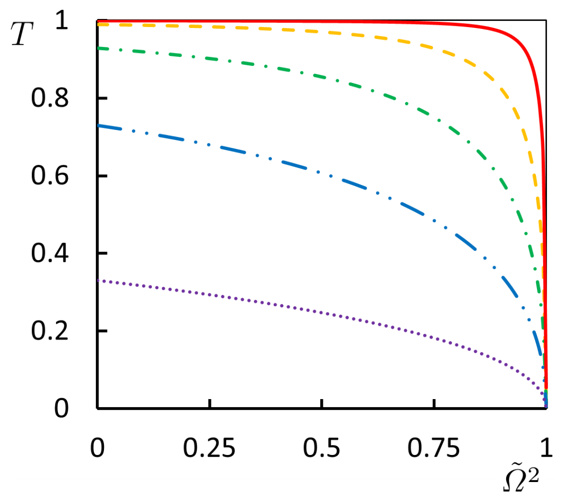

FIG. 6. Frequency dependence of the transmission coefficient T for $c_1 = c_2$ and $d_1/m_1 = d_2/m_2$. Results for m_2/m_1 equal to 1.1 (solid line), 1.5 (dashed line), 3 (dash dotted line), 10 (dash double dotted line), and 100 (dotted line) are shown.

Additionally, we note that in the case $d_1 = d_2 = 0$ and either $m_1 = m_2$ or $c_1 = c_2$, the transmission coefficient can be represented in terms of group velocities as

$$T = \frac{4g_1(\Omega)g_2(\Omega)}{[g_1(\Omega) + g_2(\Omega)]^2}. \tag{60}$$

We note that similar formula is valid for plane acoustic and electromagnetic waves, provided that the group velocities are replaced by sound speeds or by speeds of light (see, e.g., [5]).

Thus, in the case of equal minimal frequencies, the transmission coefficient, T, depends on the ratio of masses m_1/m_2 in exactly the same way as on the ratio of stiffness c_2/c_1. We also note that the function $T(\tilde{\Omega}^2, m_1/m_2, c_1/c_2)$ is exactly the same for systems with and without elastic foundation.

2. Equal maximal frequencies

We consider the case

$$\frac{4c_1 + d_1}{m_1} = \frac{4c_2 + d_2}{m_2}. \tag{61}$$

Under condition (61) formula (58) reduces to

$$T = 4\frac{m_1}{m_2}\tilde{\Omega}(1 - \tilde{\Omega}^2)\sqrt{\left(\frac{m_1}{m_2} - 1\right)\tilde{\Omega}_t^2 + \tilde{\Omega}^2}$$
$$\left[(1 - \tilde{\Omega}^2)\left(\frac{m_1}{m_2}\tilde{\Omega} + \sqrt{\left(\frac{m_1}{m_2} - 1\right)\tilde{\Omega}_t^2 + \tilde{\Omega}^2}\right)^2 + \left(\frac{m_1}{m_2} - 1\right)^2(\tilde{\Omega}^2 - \tilde{\Omega}_t^2)^2\right]^{-1},$$
$$\tilde{\Omega}_t^2 = \frac{c_2 m_1 - c_1 m_2}{c_1(m_1 - m_2)}. \tag{62}$$

Analysis of formula (62) shows that frequency dependence of the transmission coefficient can be either nonmonotonic or monotonically increasing. For $c_1 \neq c_2$ the transmission coefficient increases from zero value at $\tilde{\Omega} = 0$ to the maximum and then monotonically decreases toward zero value at $\tilde{\Omega} = 1$. For $c_1 = c_2$ the formula (62) takes the form

$$T = \frac{4\tilde{\Omega}\sqrt{\frac{m_1}{m_2} - 1 + \tilde{\Omega}^2}}{\frac{m_1}{m_2} - 1 + 2\tilde{\Omega}^2 + 2\tilde{\Omega}\sqrt{\frac{m_1}{m_2} - 1 + \tilde{\Omega}^2}}. \tag{63}$$

It is seen that the transmission coefficient is not equal to zero at $\tilde{\Omega} = 1$. On the contrary, it has the maximal value at this point.

C. Intersecting spectra

In the present subsection, we consider the case when spectra of chains 1 and 2 intersect with each other, i.e., either

$$\frac{d_1}{m_1} < \frac{d_2}{m_2} < \frac{4c_1 + d_1}{m_1} < \frac{4c_2 + d_2}{m_2} \tag{64}$$

or

$$\frac{d_2}{m_2} < \frac{d_1}{m_1} < \frac{4c_2 + d_2}{m_2} < \frac{4c_1 + d_1}{m_1}. \tag{65}$$

We show that in these cases the number of dimensionless arguments of the transmission coefficient in formula (34) can be reduced by one.

Without loss of generality we consider the case (64), corresponding to

$$\Omega_{\mathrm{low}}^2 = \frac{d_2}{m_2}, \qquad \Omega_{\mathrm{high}}^2 = \frac{4c_2 + d_2}{m_2}. \tag{66}$$

Similar results in the case (65) can be obtained by permutation of indices 1,2. Rewriting the expression (19) for the transmission coefficient in terms of the dimensionless frequency $\tilde{\Omega}$, defined by formula (33), we obtain

$$T = T\left(\tilde{\Omega}^2, \frac{m_1}{m_2}, \frac{4c_2(m_1 - m_2)\tilde{\Omega}_t^2}{d_1 m_2 - d_2 m_1}, \left[\frac{m_1}{m_2} - 1\right]\tilde{\Omega}_t^2\right),$$
$$\tilde{\Omega}_t^2 = \frac{\Omega_t^2 - \Omega_{\mathrm{low}}^2}{\Omega_{\mathrm{high}}^2 - \Omega_{\mathrm{low}}^2} = \frac{m_1(d_1 m_1 - d_2 m_1)}{(m_1 - m_2)(4c_1 m_2 + d_1 m_2 - d_2 m_1)}. \tag{67}$$

The explicit dependence is omitted for brevity. Formula (67) shows that as in the previous case of nested spectra, the transmission coefficient depends on four dimensionless parameters. Typical frequency dependence of the transmission coefficient is shown by a dashed line in Fig. 2.

D. Identical spectra

In this subsection, we consider the case when dispersion relations of chains 1 and 2 coincide ($\omega_1 = \omega_2$). This is possible provided that

$$\frac{m_1}{m_2} = \frac{c_1}{c_2} = \frac{d_1}{d_2} = \gamma_{**}. \tag{68}$$

Simplifying formula (19) using conditions (68), we obtain

$$T = \frac{T_0(\gamma_{**})\left(1 - \tilde{\Omega}^2\right)}{1 - T_0(\gamma_{**})\tilde{\Omega}^2}, \qquad T_0(\gamma_{**}) = \frac{4\gamma_{**}}{(\gamma_{**} + 1)^2}. \tag{69}$$

Then the transmission coefficient depends on two dimensionless parameters: $\tilde{\Omega}$ and γ_{**}. It is seen that the transmission

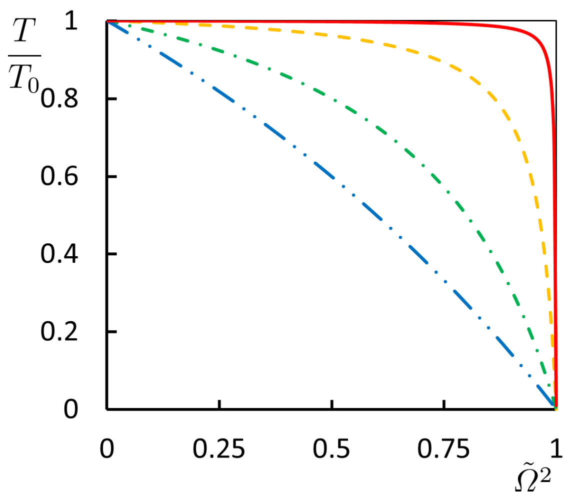

FIG. 7. Frequency dependence of the transmission coefficient $T/T_0(\gamma_{**})$ for two chains with identical spectra [see formula (68)]. Results for γ_{**} equal to 1.1 (solid line), 1.5 (dashed line), 3 (dash dotted line), and 10 (dash double dotted line) are shown.

coefficient has maximum value of T_0 at $\tilde{\Omega} = 0$ and monotonically decreases toward zero value at $\tilde{\Omega} = 1$. The maximum value of the transmission coefficient tends to zero as γ_{**} tends to infinity ($T_0 \sim 4/\gamma_{**}$). Frequency dependence of the normalized transmission coefficient $T/T_0(\gamma_{**})$ for different values of γ_{**} is shown in Fig. 7. The figure shows that the normalized transmission coefficient tends to become independent on the frequency (and equal to unity) for $\gamma_{**} \to 1$. For $\gamma_{**} \gg 1$, the transmission coefficient depends on the squared frequency almost linearly, i.e., $T/T_0 \approx 1 - \tilde{\Omega}^2$.

VIII. CONCLUSIONS

We have shown that by adding the on-site potential (elastic foundation) one can qualitatively change the frequency dependence of the transmission coefficient. In chains without elastic foundation, the transmission coefficient monotonically decreases with increasing frequency. In chains with elastic foundation, the frequency dependence is either monotonically decreasing or nonmonotonic, or even monotonically increasing. The conditions corresponding to these three qualitatively different cases has been derived. It was shown, in particular, that qualitative type of the dependence is determined by the way how spectra of the two chains intersect with each other. For example, the transmission coefficient monotonically increases with frequency provided that the highest frequencies of the two chains are equal [see formula (37)]. Presented qualitative results may be important, e.g., for understanding of transmission through the interface between two lattices with several particles per unit cell (and several branches of the dispersion relation), because their spectra may intersect in many different ways.

It was shown that the elastic foundation can make the interface totally transparent (the transmission coefficient is equal to unity). The acoustic transparency is observed at frequency, given by formula (40). In the vicinity of this frequency the transmission coefficient is close to one, and therefore the interface is almost transparent. Mathematical explanation of the acoustic transparency is that equations of motion for both chains have the same exact solution in the form of an infinite harmonic wave. This wave propagates through the interface without any reflection or distortion. Similar behavior is observed for wave packets. The amplitudes of the displacements/velocities in the incident and transmitted wave packets are equal, while widths of these wave packets are different. The ratio of widths is inversely proportional to the ratio of group velocities of the two chains.

One of the goals of the present paper was to analyze the influence of parameters of the two chains on the transmission coefficient. The complete analysis is quite cumbersome because even if we set $c_{12} = c_1$, the problem still contains seven parameters: wave frequency, two masses, and four stiffnesses. Using dimensionalization, we have reduced the number of parameters to four.

We note that the effect of nonlinearity of interparticle interactions and on-site potential on the transmission coefficient have not been considered in the present paper. We assume that since the transmission of wave packets through the interface is a relatively fast process, a weak nonlinearity may not have enough time to manifest (similarly to quasiballistic energy transfer [7,10,43] and interfacial heat transfer [44] in weakly nonlinear lattices). Therefore we believe that the presented results should be valid for anharmonic systems at least in the weakly nonlinear limit. However, determining the limits of applicability of the linear model, considered in the present paper, requires a separate study.

From a practical point of view, the presented results may serve, in particular, for managing energy transport and interfacial thermal resistance (Kapitza resistance [16]) in low-dimensional systems at the nanoscale, e.g., carbyne, nanowires, graphene, and other one- and two-dimensional materials. The low-dimensional systems are usually located at the substrate, which acts as the elastic foundation. Our results show that by chooosing properties of the elastic foundation one may control the transmission coefficient and therefore the interfacial thermal resistance. We refer to paper [17] for a comprehensive review on the state of the art in the interfacial thermal resistance problem and to the recent paper [44] for analytical expressions for the Kapitza resistance in harmonic one-dimensional chains.

ACKNOWLEDGMENTS

The author is grateful to the late Prof. Dmitry Anatolievich Indeitsev (02.12.1948–28.12.2022) for teaching him about the beauty of waves [37] and science in general. The author is also gateful to S.N. Gavrilov, S.V. Dmitriev, A.B. Freidin, E.A. Ivanova, A.M. Krivtsov, S.D. Liazhkov, G.S. Mishuris, and E.V. Shishkina for useful discussions. The work was supported by the Russian Science Foundation (Grant No. 21-71-10129).

APPENDIX A: SOME CHARACTERISTICS OF A WAVE PACKET

We calculate values u_n^2, v_n^2, $\varepsilon_{n+\frac{1}{2}}^2$, $u_n u_{n+1}$, $h_{n+\frac{1}{2}}$ for a wave packet, propagating in the chain 2 ($n \geqslant 0$), using the following expression for the transmitted wave packet:

$$u_n = B(\beta na, \beta t)\sin(k_2 n - \Omega t), \qquad \beta \ll 1. \tag{A1}$$

Squares of displacements and velocities are equal to

$$\begin{aligned} u_n^2 &= \frac{1}{2}B^2(\beta na, \beta t)[1 - \cos(2k_2 n - 2\Omega t)], \\ v_n^2 &\approx \frac{1}{2}B^2(\beta na, \beta t)\Omega^2[1 - \cos(2k_2 n - 2\Omega t)]. \end{aligned} \tag{A2}$$

Here and below the sign "≈" means that the terms, vanishing as $\beta \to 0$, are neglected. Squared deformations of the bonds and products of displacements of the neighboring particles are equal to

$$\begin{aligned} \varepsilon_{n+\frac{1}{2}}^2 &\approx 2B^2(\beta na, \beta t)\sin^2\frac{k_2}{2}[1 + \cos((2n+1)k_2 - 2\Omega t)], \\ u_n u_{n+1} &\approx \frac{1}{2}B^2(\beta na, \beta t)[\cos k_2 - \cos((2n+1)k_2 - 2\Omega t)]. \end{aligned} \tag{A3}$$

The local energy flux, defined by formula (20), is equal to

$$h_{n+\frac{1}{2}} \approx \frac{1}{2}m_2\Omega^2 g_2 B^2(\beta na, \beta t)[1 + \cos((2n+1)k_2 - 2\Omega t)]. \tag{A4}$$

The local energy is equal to

$$\begin{aligned} e_n &= \frac{1}{2}m_2 v_n^2 + \frac{c_2}{4}\left(\varepsilon_{n+\frac{1}{2}}^2 + \varepsilon_{n-\frac{1}{2}}^2\right) + \frac{1}{2}d_2 u_n^2 \\ &\approx \frac{1}{2}m_2\Omega^2 B^2(\beta na, \beta t)\left(1 + \frac{m_2\Omega^2 - d_2}{m_2\Omega^2}\right. \\ &\quad \left.\times \cos\frac{k_2}{2}\cos(2k_2 n - 2\Omega t)\right). \end{aligned} \tag{A5}$$

It is seen that all quantities considered above are represented as a sum of a slowly changing function, proportional to the squared envelope B^2, and an oscillating function. When these quantities are integrated over large time, the oscillating part can be neglected, provided that β is sufficiently small. Then

$$\begin{aligned} e_n &\sim \frac{1}{2}m_2\Omega^2 B^2(\beta na, \beta t), \\ h_{n+\frac{1}{2}} &\sim \frac{1}{2}m_2\Omega^2 g_2 B^2(\beta na, \beta t), \\ u_n^2 &\sim \frac{1}{2}B^2(\beta na, \beta t), \quad v_n^2 \sim \frac{1}{2}B^2(\beta na, \beta t)\Omega^2, \\ u_n u_{n+1} &\sim \frac{1}{2}B^2(\beta na, \beta t)\cos k_2, \end{aligned} \tag{A6}$$

where the "∼" sign means that functions have the same integral for small β:

$$f_1(t) \sim f_2(t) \quad \Leftrightarrow \quad \int_0^\infty f_1(\tau)\,d\tau \approx \int_0^\infty f_2(\tau)\,d\tau. \tag{A7}$$

From formula (A6) it follows, in particular, that the total energy flux in chain 2 is approximately equal to $E_2(\infty)g_2$.

APPENDIX B: CONSTITUTIVE RELATION FOR THE "FORCE" CHANGING THE TOTAL FLUX

In this Appendix, we derive the constitutive relation for the r.h.s. of the equation

$$h(\infty) - h(0) = \int_0^\infty \mathcal{F} dt, \tag{B1}$$

where

$$\begin{aligned} \mathcal{F} &= \frac{a}{2}(c_2 - c_1)\left(v_0^2 - \frac{d_2}{m_2}u_0^2\right) \\ &\quad + \frac{a(m_1 - m_2)}{2m_1 m_2}c_1^2\varepsilon_{-\frac{1}{2}}^2 + \frac{ac_1}{2}\left(\frac{d_1}{m_1} - \frac{d_2}{m_2}\right)u_0 u_{-1}. \end{aligned} \tag{B2}$$

The main goal is to represent the r.h.s. of formula (B1) in terms of energy of the transmitted wave packet $E_2(\infty)$.

We use equations of energy balance for chain 2 and for the particle 0:

$$\dot{E}_2 = h_{-\frac{1}{2}}/a, \qquad a\dot{e}_0 = h_{-\frac{1}{2}} - h_{\frac{1}{2}}, \tag{B3}$$

where e_0 is the total energy per particle 0, defined by (50). Additionally, we use the following identities relating quantities corresponding to chains 1 and 2

$$\begin{aligned} \int_0^\infty v_0^2 dt &= (u_0 v_0)|_0^\infty - \int_0^\infty u_0\dot{v}_0 dt = \\ &= -\frac{1}{m_2}\int_0^\infty u_0\left(F_{\frac{1}{2}} - F_{-\frac{1}{2}} - d_2 u_0\right)dt, \\ F_{-\frac{1}{2}}^2 &= F_{\frac{1}{2}}^2 + (m_2\dot{v}_0 + d_2 u_0)\left(m_2\dot{v}_0 + d_2 u_0 - 2F_{\frac{1}{2}}\right). \end{aligned} \tag{B4}$$

Here in the first identity the nonintegral term is neglected, assuming that there is no localization of energy at the interface. The second identity is obtained by combining squared equation of motion (12) for particle 0 with the same equation multiplied by $F_{\frac{1}{2}}$.

We integrate equations (B3) and the second equation in (B4) over time:

$$\begin{aligned} &aE_2(\infty) = \int_0^\infty h_{-\frac{1}{2}} dt = \int_0^\infty h_{\frac{1}{2}} dt, \\ &\int_0^\infty (m_2 v_0^2 - d_2 u_0^2) dt = -\int_0^\infty u_0\left(F_{\frac{1}{2}} - F_{-\frac{1}{2}}\right)dt, \\ &\int_0^\infty F_{-\frac{1}{2}}^2 dt = \int_0^\infty F_{\frac{1}{2}}^2 dt + \\ &+ \int_0^\infty (m_2\dot{v}_0 + d_2 u_0)\left(m_2\dot{v}_0 + d_2 u_0 - 2F_{\frac{1}{2}}\right)dt. \end{aligned} \tag{B5}$$

Further, we show that all integrals in this formula are proportional to $E_2(\infty)$. Note that formulas (B5) are exact and valid under arbitrary initial conditions (provided that $(u_0 v_0)|_0^\infty$).

We assume that the energy is transferred to chain 2 by a wave packet with frequency Ω and unknown envelope $B(\beta na, \beta t)$:

$$u_n = B(\beta na, \beta t)\sin(k_2 n - \Omega t), \quad n \geqslant 0, \quad |\beta| \ll 1. \tag{B6}$$

According to the definition (B1), the "force" $\mathcal{F}$ linearly depends on u_0^2, v_0^2, $\varepsilon_{-\frac{1}{2}}^2$, and $u_0 u_{-1}$. The first two of these quantities are related to the envelope of the wave packet (B6) as (see Appendix A)

$$u_0^2 \sim u_1^2 \sim \frac{1}{2}B^2(0,\beta t), \qquad v_0^2 \sim \frac{1}{2}\Omega^2 B^2(0,\beta t), \tag{B7}$$

where the "∼" sign means that the functions have the same integral for small β [see definition (A7)]. The quantities u_0u_{-1}, $\varepsilon^2_{-\frac{1}{2}}$ are represented in terms of the envelope function using the following relations, derived from (B5) and (B6):

$$\begin{aligned} c_1u_0u_{-1} &\sim (c_1+c_2+d_2)u_0^2 - c_2u_0u_1 - m_2v_0^2,\\ c_1^2\varepsilon^2_{-\frac{1}{2}} &\sim c_2^2\varepsilon^2_{\frac{1}{2}} = c_2^2\big(u_0^2+u_1^2-2u_0u_1\big),\\ u_0u_1 &\sim \frac{1}{2}B^2(0,\beta t)\cos k_2. \end{aligned} \tag{B8}$$

We note that under assumption (B6), the fourth formula from (B5) yields $F^2_{-\frac{1}{2}} \sim F^2_{\frac{1}{2}}$.

Similarly, the local flux $h_{\frac{1}{2}}$ is represented as (see Appendix A)

$$h_{\frac{1}{2}} \sim \frac{1}{2}m_2\Omega^2 g_2 B^2(0,\beta t). \tag{B9}$$

Then formulas (B7), (B8), and (B9) show that u_0^2, v_0^2, $\varepsilon^2_{-\frac{1}{2}}$, u_0u_{-1}, and $h_{\frac{1}{2}}$ are represented in terms of $B^2(0,\beta t)$. In turn, B^2 is related to the energy E_2 via the first formula from (B5) and formula (B9):

$$\int_0^\infty B^2(0,\beta t)\,dt \approx \frac{2aE_2(\infty)}{m_2\Omega^2 g_2}. \tag{B10}$$

This formula allows to represent all quantities in the expression for integral of $\mathcal{F}$ in terms of the energy $E_2(\infty)$. Using (B10) and formulas (B7) and (B8), we obtain

$$\begin{aligned} \int_0^\infty \left(v_0^2 - \frac{d_2}{m_2}u_0^2\right)dt &\approx \left(\Omega^2 - \frac{d_2}{m_2}\right)\frac{aE_2(\infty)}{m_2\Omega^2 g_2},\\ \int_0^\infty c_1^2\varepsilon^2_{-\frac{1}{2}}dt &\approx \left(\Omega^2 - \frac{d_2}{m_2}\right)\frac{c_2aE_2(\infty)}{\Omega^2 g_2},\\ \int_0^\infty c_1u_0u_{-1}dt &\approx \left(\frac{2c_1+d_2}{m_2} - \Omega^2\right)\frac{aE_2(\infty)}{2\Omega^2 g_2}. \end{aligned} \tag{B11}$$

Then formulas (B1) and (B11) yield

$$\int_0^\infty \mathcal{F}dt \approx G(\Omega)E_2(\infty), \tag{B12}$$

where $G(\Omega)$ is given by formula (30).

[1] L. Rayleigh, Theory of Sound, Band II, McMillan, London, 1894.
[2] F. Bonetto, J. L. Lebowitz, and L. Rey-Bellet, Fourier's law: a challenge to theorists, Math. Phys., 128 (2000).
[3] S. Lepri, R. Livi, and A. Politi, Thermal conduction in classical low-dimensional lattices, Phys. Rep. **377**, 1 (2003).
[4] A. Dhar, Heat transport in low-dimensional systems, Adv. Phys., **57**, 457 (2008).
[5] G. Chen, Nanoscale energy transport and conversion: a parallel treatment of electrons, molecules, phonons, and photons, Oxford university press, 2005.
[6] R. Anufriev, S. Gluchko, S. Volz, and M. Nomura, Quasi-ballistic heat conduction due to levy phonon flights in silicon nanowires, ACS Nano, **12**, 11928 (2018).
[7] V. A. Kuzkin and A. M. Krivtsov, Ballistic resonance and thermalization in Fermi-Pasta-Ulam-Tsingou chain at finite temperature, Phys. Rev. E **101**, 042209 (2020).
[8] V. Kannan, A. Dhar, and J. L. Lebowitz, Nonequilibrium stationary state of a harmonic crystal with alternating masses, Phys. Rev. E **85**, 041118 (2012).
[9] V. A. Kuzkin, Unsteady ballistic heat transport in harmonic crystals with polyatomic unit cell, Continuum Mech. Thermodyn. **31**, 1573 (2019).
[10] S. D. Liazhkov and V. A. Kuzkin, Unsteady two-temperature heat transport in mass-in-mass chains, Phys. Rev. E **105**, 054145 (2022).
[11] A. M. Krivtsov, Heat transfer in infinite harmonic one dimensional crystals, Dokl. Phys. **60**, 407 (2015).
[12] A. A. Sokolov, A. M. Krivtsov, W. H. Müller, and E. N. Vilchevskaya, Change of entropy for one-dimensional ballistic heat equation—sinusoidal initial perturbation, Phys. Rev. E **99**, 042107 (2019).
[13] A. S. Murachev, A. M. Krivtsov, and D. V. Tsvetkov, Thermal echo in a one-dimensional harmonic crystal, J. Phys.: Condens. Matter **31**, 095702 (2019).
[14] M. Terraneo, M. Peyrard, and G. Casati, Controlling the Energy Flow in Nonlinear Lattices: A Model for a Thermal Rectifier, Phys. Rev. Lett. **88**, 094302 (2002).
[15] B. Li, L. Wang, and G. Casati, Phys. Rev. Lett. **93**, 184301 (2004).
[16] P. L. Kapitza, Heat Transfer and Superfluidity of Helium II, Phys. Rev. **60**, 354 (1941).
[17] J. Chen, X. Xu, J. Zhou, and B. Li, Interfacial thermal resistance: Past, present, and future, Rev. Mod. Phys. **94**, 025002 (2022).
[18] C. Steinbrüchel, The scattering of phonons of arbitrary wavelength at a solid-solid interface: Model calculation and applications, Z. Phys. B: Condens. Matter **24**, 293 (1976).
[19] M. E. Lumpkin, W. M. Saslow, and W. M. Visscher, One-dimensional Kapitza conductance: Comparison of the phonon mismatch theory with computer experiments, Phys. Rev. B **17**, 4295 (1978).
[20] H. Jex, The transmission and reflection of acoustic and optic phonons from a solid-solid interface treated in a linear chain model, Z. Phys. B **63**, 91 (1986).
[21] R. R. Kakodkar and J. P. Feser, A framework for solving atomistic phonon-structure scattering problems in the frequency domain using perfectly matched layer boundaries, J. Appl. Phys. **118**, 094301 (2015).
[22] C. A. Polanco, C. B. Saltonstall, P. M. Norris, P. E. Hopkins, and A. W. Ghosh, Impedance matching of atomic thermal interfaces using primitive block decomposition, Nanoscale Microscale Thermophys. **17**, 263 (2013).

[23] C. B. Saltonstall, C. A. Polanco, J. C. Duda, A. W. Ghosh, P. M. Norris, and P. E. Hopkins, Effect of interface adhesion and impurity mass on phonon transport at atomic junctions, J. Appl. Phys. **113**, 013516 (2013).

[24] G. Xiong, J. S. Wang, D. Ma, and L. Zhang, Dramatic enhancement of interfacial thermal transport by mass-graded and coupling-graded materials, Europhys. Lett. **128**, 54007 (2020).

[25] L. Yang, X. Wan, D. Ma, Y. Jiang, and N. Yang, Maximization and minimization of interfacial thermal conductance by modulating the mass distribution of the interlayer, Phys. Rev. B **103**, 155305 (2021).

[26] D. Ma, Y. Xing, and L. Zhang, Reducing interfacial thermal resistance by interlayer, J. Phys.: Condens. Matter **35**, 053001 (2022).

[27] Yu. A. Kosevich, Multichannel propagation and scattering of phonons and photons in lowdimension nanostructures, Phys. Usp. **51**, 848 (2008).

[28] B. Hu, D. He, L. Yang, and Y. Zhang, Asymmetric heat conduction through a weak link, Phys. Rev. E **74**, 060101 (2006).

[29] D. He, S. Buyukdagli, and B. Hu, Origin of negative differential thermal resistance in a chain of two weakly coupled nonlinear lattices, Phys. Rev. B **80**, 104302 (2009).

[30] A. M. Krivtsov, Dynamics of matter and energy, ZAMM – J. Appl. Math. Mech. **103**, e202100496 (2022).

[31] J. A. Baimova, N. M. Bessonov, and A. M. Krivtsov, Motion of localised disturbances in scalar harmonic lattices, Phys. Rev. E **107**, 065002 (2023).

[32] J. W. Strutt, Some general theorems relating to vibrations, Proc. London Math. Soc. **s1-4**, 357 (1873).

[33] S. Leibovich and A. R. Seebass (ed.), *Nonlinear Waves* (Cornell University Press, Ithaca and London, 1974).

[34] A. Mielke, Macroscopic behavior of microscopic oscillations in harmonic lattices via Wigner-Husimi transforms, Arch. Rational Mech. Anal. **181**, 401 (2006).

[35] P. K. Schelling, S. R. Phillpot, and P. Keblinski, Phonon wavepacket dynamics at semiconductor interfaces by molecular-dynamics simulation, Appl. Phys. Lett. **80**, 2484-2486 (2002).

[36] S. H. Simon, *The Oxford Solid State Basics, Solutions to Exercises* (Clarendon Press, Oxford, 2015).

[37] D. Indeitsev, N. Kuznetsov, O. Motygin, and Y. Mochalova, Localization of linear waves, St. Petersburg University, St. Petersburg (2007) (in Russian).

[38] A. Abramyan, V. Andreyev, and D. Indejtchev, Resonance oscillations of infinite and finite elastic structures with inclusions, J. Acoust. Soc. Am. **95**, 3007 (1994).

[39] I. V. Andrianov, V. V. Danishevs'kyy, and A. L. Kalamkarov, Vibration localization in one-dimensional linear and nonlinear lattices: discrete and continuum models, Nonlinear Dyn. **72**, 37 (2012).

[40] E. V. Shishkina, S. N. Gavrilov, and Yu. A. Mochalova, Non-stationary localized oscillations of an infinite Bernoulli-Euler beam lying on the Winkler foundation with a point elastic inhomogeneity of time-varying stiffness, J. Sound Vib. C **440**, 174 (2019).

[41] G. S. Mishuris, A. B. Movchan, and L. I. Slepyan, Localized waves at a line of dynamic inhomogeneities: General considerations and some specific problems, J. Mech. Phys. Solids **138**, 103901 (2020).

[42] E. V. Shishkina and S. N. Gavrilov, Unsteady ballistic heat transport in a 1D harmonic crystal due to a source on an isotopic defect, Continuum Mech. Thermodyn., **35**, 431 (2023).

[43] E. A. Korznikova, V. A. Kuzkin, A. M. Krivtsov, X. Daxing, V. A. Gani, A. A. Kudreyko, and S. V. Dmitriev, Equilibration of sinusoidal modulation of temperature in linear and nonlinear chains, Phys. Rev. E **102**, 062148 (2020).

[44] J. Paul and O. V. Gendelman, Kapitza resistance at a domain boundary in linear and nonlinear chains, Phys. Rev. E **104**, 054119 (2021).